

Spinor bosons realization of the SU(3) Haldane phase with adjoint representation

Junjun Xu*

Institute of Theoretical Physics, University of Science and Technology Beijing, Beijing 100083, China

(Dated: July 10, 2023)

The SU(3) Haldane phase with adjoint representation provides the simplest non-trivial symmetry-protected topological phases in the SU($N > 2$) spin chains for which a gapped system has been predicted. In this letter, I show how to realize this phase in a two-species spinor Bose gas. The proposed system consists of two intertwined species-dependent zigzag optical lattices with the two species labeling the quark and antiquark states of SU(3) symmetry. The Haldane phase is found connected to a position at which both the string order and entanglement spectrum degeneracy are absent, signaling the appearance of a critical point. I show how to understand this absence by a ground-state ansatz.

The Haldane conjecture that predicts a gapped ground state in an SU(2) integer-spin antiferromagnetic Heisenberg spin chain [1–3] has reshaped our understanding and classification of quantum matters, which eventually leads to the discovery of the symmetry-protected topological (SPT) phases [4–6]. Recently, theoretical progress in this direction generalizes the Haldane conjecture to SU(N) symmetric representations, and finds a gapless ground state when the number of boxes in the Young diagram p is coprime with N , which is connected to the SU(N)₁ Wess-Zumino-Witten conformal field theory, while for other representations field theory calculations predict a finite mass gap [7, 8]. Interpretations about this mass gap include the existence of spinon confinement [9–11], and more recently the fractional topological excitations called instantons [12].

Compared to the SU(2) case, the richer representations of the SU(N) symmetry can give rise to new features in their gapped states. For example, the SU(N) SPT phases can be protected by the $Z_N \times Z_N$ symmetry, and have $N - 1$ distinct non-trivial classes, corresponding to different elements of the second cohomology group $H^2(Z_N \times Z_N, U(1)) = \mathbb{Z}_N$, which can be revealed by the representations of different edge states [13, 14]. At the same time, the ground state of the SU(N) system can have degeneracies if these non-trivial classes are symmetrically connected.

On the numerical front, the minimal model to check the above SU(N) physics is to consider the SU(3) symmetry. For the symmetric representation with Young diagram [3 0 0], large-scale density matrix renormalization group (DMRG) calculations confirm recently the ground state with a gap around $0.04J$ [15], however, more recent tensor-network results find this state belongs to the trivial SPT phase [16]. For non-symmetric representations, recent Monte Carlo simulations together with field theory calculations show there is always a gapped phase in the SU(3) self-conjugate representations. Different from the SU(2) case, the flavor-wave calculation shows six Goldstone bosons with two different velocities, and the topological angle becomes non-trivial with a spontaneously broken parity symmetry for an odd number of boxes [17].

So the minimal model with non-trivial SU(N) physics would be the SU(3) system with adjoint representation [2 1 0]. In this system, the edge states of the two sides can be in the representation [1 0 0] – [1 1 0] or [1 1 0] – [1 0 0], corresponding to the two classes of the SU(3) SPT phases. Thus each class breaks the inversion symmetry, and has different chiralities [18, 19]. The Affleck-Kennedy-Lieb-Tasaki (AKLT) state and its parent Hamiltonian have been constructed, and this system is found protected by the $Z_3 \times Z_3$ symmetry with a doubly degenerate ground state [13].

On the experimental front, the cold atomic system has become the promising candidate for realizing the SU(N) SPT phases [20]. Progresses have been pushing forward to the SU(N) physics using alkali-earth atoms. Since all the experimentally accessible spinful alkali-earth atoms are fermionic, proposals in this system are focusing on the SU(N) SPT phases with N even, and with a unique ground state [21–23].

In this letter, I take on an alternative route by considering a bosonic system, and give the first experimentally realizable proposal for the non-trivial Haldane phase in a minimal SU(3) adjoint representation in this system. I make use of a Schwinger bosons representation [24–26], and consider two species of bosons a and b , both in three substates of their hyperfine spin $F = 2$ state. The Hamiltonian of the SU(3) adjoint representation spin chain can be mapped as

$$H = \sum_{\langle ij \rangle, \sigma, \sigma'} \left[t \left(a_{i, \sigma}^\dagger a_{j, \sigma'}^\dagger a_{j, \sigma} a_{i, \sigma'} + b_{i, \sigma}^\dagger b_{j, \sigma'}^\dagger b_{j, \sigma} b_{i, \sigma'} \right) - g_0 \left(a_{i, \sigma}^\dagger b_{j, -\sigma}^\dagger b_{j, -\sigma'} a_{i, \sigma'} + b_{i, -\sigma}^\dagger a_{j, \sigma}^\dagger a_{j, \sigma'} b_{i, -\sigma'} \right) \right] \quad (1)$$

where the summation is over the nearest sites and σ corresponds to different hyperfine states. Here the positive intraspecies interaction t accounts for the suppression of hopping for the quarks or antiquarks on the nearest sites, which will be explained in the following. The g_0 term comes from the scattering at total hyperfine spin $F = 0$ channel, which keeps the quark-antiquark pair in the singlet space with $[1 1 1] = \sum_{\sigma} a_{\sigma}^\dagger b_{-\sigma}^\dagger |0\rangle$. Here the spin-2 bosons are crucial, as the Clebsch-Gordon coef-

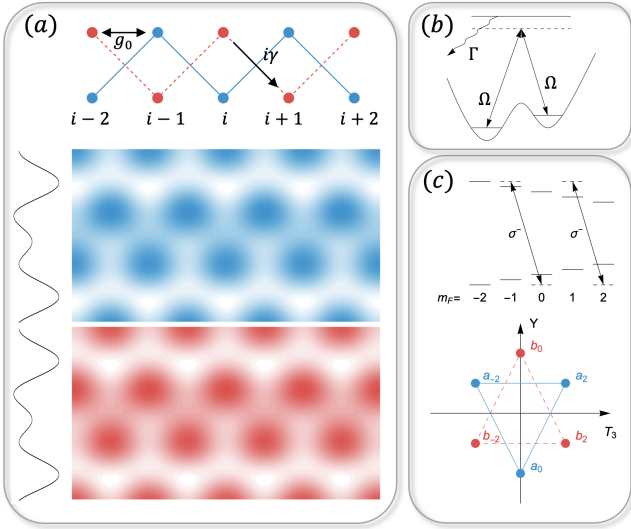


FIG. 1. An illustration of the experimental implementation. (a) The species-dependent optical potential is used to construct two intertwined zigzag lattices, where each species is composed of three degenerate states in the hyperfine $F = 2$ state. The hopping in each species is imaginary $i\gamma$, and the interspecies interaction strength g_0 depends on the overlap of their distribution that is on the same leg. (b) The effective imaginary hopping can be induced by a two-photon Raman process, which couples the states in the tilted lattice to a higher energy level with a decay rate Γ . (c) By combining the magnetic field and σ^- polarized lasers, the three lowest hyperfine states in the spin-2 bosons a and b are picked up, realizing the quark and antiquark states of the SU(3) symmetry.

ficients for two spin-1 atoms will lead to a sign change for different scattering states [27], which will break this quark-antiquark singlet state. To reach this Hamiltonian, we need to tune the interaction to be within the strong interacting limit at filling $n = 1$ for each species [28], and without the interspecies scattering other than $F = 0$ channel. These could be realized by using optical or microwave Feshbach resonances [29–31].

The experimental realization can be illustrated in Fig. 1. We create a species-dependent zigzag optical lattice by combining the use of lasers with three different wavelengths λ_0 which is blue detuned from species a and red detuned from species b , $\lambda_r = \sqrt{2}\lambda_0$ which is red detuned from the two species, and $\lambda_b = \lambda_0/\sqrt{2}$ which is blue detuned from the two species [32–34]. Two sets of counter propagating λ_0 lasers create a species dependent diagonal square optical lattice $V_{dep} = V_0 \cos(\frac{k_0x+k_0y}{\sqrt{2}})^2 + V_0 \cos(\frac{k_0x-k_0y}{\sqrt{2}})^2$ with $k_0 = 2\pi/\lambda_0$. A periodic modulation is added along the y axis to separate each two-leg system and reduce the spin-mixing interaction at the same site with $V_y = V_0 \cos(k_by + \pi/2 + \phi)^2 - V_0 \cos(k_ry + \pi/4)^2$, as illustrated in the solid curve in Fig. 1a, where we have added a small phase difference ϕ to create a tilted

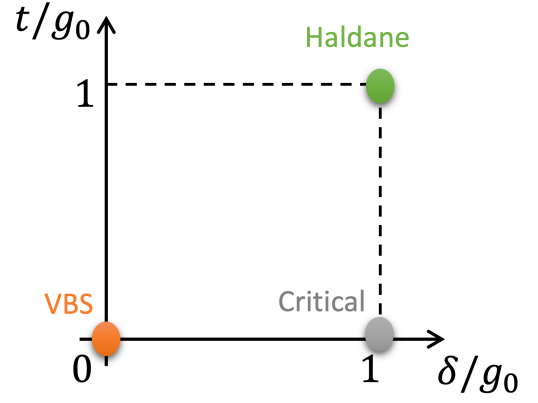


FIG. 2. Characteristic phases in our parameter regime. The different phases are connected except at the critical point for $t/g_0 = 0$ and $\delta/g_0 = 1$.

lattice [35–37]. A demonstration of the realized species-dependent optical lattice for atoms a (blue) and b (red) is shown in Fig. 1a, where the denser color corresponds to a lower trap depth. Here the tilted lattices prevent the hopping of atoms at the nearest sites within each species, and at the same time help to include an effective imaginary hopping. We propose to use two Raman lasers with Rabi frequency Ω to couple the tilted lattices to the same higher energy level which has a decay rate Γ as in Fig. 1b. The detuning and decay rate can be tuned to be sufficiently large so that by adiabatic elimination we end up with an imaginary hopping $i\gamma \propto i\Omega^2/\Gamma$ in the zig-zag lattice as in Fig. 1a. By a non-Hermitian perturbation theory [38], this imaginary hopping gives rise to a positive interaction t in Eq. (1). To realize a SU(3) symmetric system within the hyperfine spin $F = 2$ states, we propose to combine the magnetic field with σ^- polarized lasers to pick up the lowest hyperfine states with $m_F = 0, \pm 2$ as shown in Fig. 1c. In this case, we can map these lowest hyperfine states a_σ and b_σ to the quark and antiquark states.

We show in Fig. 2 the characteristic phases in the parameter regime at the limit of strong on-site repulsion. To illustrate the evolution to the SU(3) Haldane phase, we include an energy shift to the left and right chiral states in the interspecies interaction with $-\sum_{\langle ij \rangle, \sigma, \sigma'} (g_0 a_{i, \sigma}^\dagger b_{j, -\sigma}^\dagger b_{j, -\sigma'} a_{i, \sigma'} + \delta b_{i, -\sigma}^\dagger a_{j, \sigma}^\dagger a_{j, \sigma'} b_{i, -\sigma'})$, where $\delta/g_0 \in [0, 1]$. As expected, a well-defined valence bond solid (VBS) state (orange) is found at $\delta = 0$ where a right chiral SU(3) singlet pair is formed at the nearest sites. By increasing t the system can adiabatically evolve to the right chiral Haldane phase. Then by increasing the energy shift δ , the left chiral Haldane state becomes involved. At $\delta/g_0 = 1$ these two chiral states become degenerate, and we arrive at a ground state SU(3) Haldane phase (green) with double degeneracy. Interestingly, we find a critical phase (gray) when evolves to the point

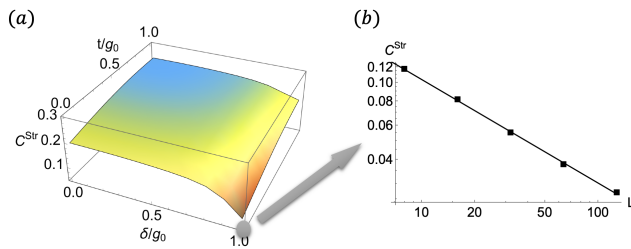


FIG. 3. (a) The string order parameter $C^{\text{Str}} = C^{\text{Str}}(L/4, 3L/4)$ as a function of intraspecies interaction t and interspecies spin-mixing energy shift δ . (b) Finite-size scaling of the string order parameter shows a power-law behavior at the critical point for $t/g_0 = 0$ and $\delta/g_0 = 1$.

at $t = 0$ and $\delta/g_0 = 1$. We explain in the following the evidence of these characteristic phases.

To confirm the qualitative phase diagram in Fig. 2, we consider the following string order parameter

$$C^{\text{Str}}(i, j) = \left\langle \Delta n_2^i e^{i\pi \sum_{i < k < j} \Delta n_2^k} \Delta n_2^j \right\rangle, \quad (2)$$

where $\Delta n_2^i = n_{a_2}^i - n_{b_{-2}}^i$ measures the particle number difference between the quark and antiquark state a_2 and b_{-2} at site i . This number difference corresponds to the charge $Q^i = T_3^i + Y^i/2$ according to the Gell-Mann-Nishijima formula, and takes values $-1, 0$, and 1 in the meson state [39, 40]. We show this string order parameter for different intraspecies interaction t and interspecies spin-mixing energy shift δ for an experimentally realizable system size $L = 16$ in Fig. 3a by DMRG calculations. To reduce the Hilbert space and lift up additional degeneracies, we consider an open system, and choose subspaces with $T_3 = 1$ and $Y = 0$. The string order decreases apparently close to $\delta/g_0 = 1$ and $t = 0$, signaling a critical regime. We further push the calculations to system size $L = 128$, the string order parameter shows a power-law behavior at this point as expected for a critical system as in Fig. 3b. We keep up to 1600 states in the DMRG calculations, and do not observe signatures of phase transition within the parameter regime.

The above results are consistent with the ground-state entanglement properties. We illustrate the evolution of the entanglement spectrum in Fig. 4 from the VBS to critical and from critical to Haldane point. To avoid boundary effects, here we consider a periodic chain and take chain length $L = 16$. The entanglement spectrum shows a well-defined 9-fold degeneracy in the VBS state in Fig. 4a, corresponding to the entanglement of two $SU(3)$ singlets appearing at the boundaries of the half system. The large entanglement gap above the nine degenerate entanglement eigenvalues is consistent with the appearance of a Haldane gap. The degeneracy is lifted up close to the critical point at $t/g_0 = 0$ and $\delta/g_0 = 1$ with this entanglement gap vanishing. This signals the appearance of a critical point. As shown in Fig. 4b,

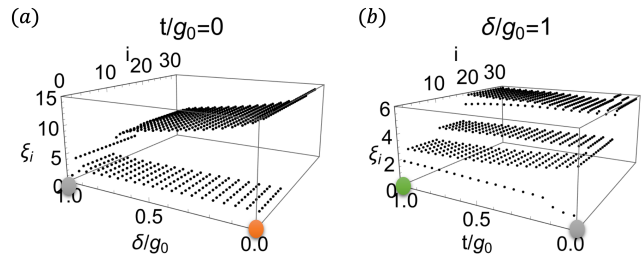


FIG. 4. Evolution of the entanglement spectrum from the VBS to critical state at $t/g_0 = 0$ in (a) and from the critical to Haldane phase at $\delta/g_0 = 1$ in (b). There is a spectrum gap above the 9th entanglement eigenvalue ξ_9 in both the VBS (orange) and Haldane (green) points. Approaching the critical point (gray) this spectrum gap closes.

deviated from the critical point the entanglement gap reopens, and the nine smallest entanglement eigenvalues gather when approaching the Haldane point. Here the absence of the 9-fold degeneracy away from the critical point is due to the finite-size effect.

To further study the physics at this critical point, we consider the reduced Hamiltonian

$$H_C = - \sum_{\langle ij \rangle, \sigma, \sigma'} \left(a_{i, \sigma}^\dagger b_{j, -\sigma}^\dagger b_{j, -\sigma'} a_{i, \sigma'} + b_{i, -\sigma}^\dagger a_{j, \sigma}^\dagger a_{j, \sigma'} b_{i, -\sigma'} \right),$$

and try to figure out what the ground state looks like. We start from the right chiral Haldane phase $|\psi_R\rangle$ as illustrated in the inset of Fig. 5, where the red and blue dots label the quark and antiquark states at site i , and the solid lines label the $SU(3)$ singlet bonds. We observe if the Hamiltonian H_C is acting on $|\psi_R\rangle$, the resulting states are a superposition of states with each quark/antiquark state connected with a single solid line. So the effects of the Hamiltonian H_C just shift these solid lines. This observation suggests the ground state of H_C might be constructed from states with fully connected singlet states.

We label each substate as $\{r_i\}$ with the quark state at site i connected to the antiquark state at site r_i , and different structures correspond to different permutations of the list from 1 to L . For example, the right chiral Haldane phase $|\psi_R\rangle$ can be labeled as $|2, 3, 4, \dots, L, 1\rangle$. The two-site system $L = 2$ is trivial, and the ground state is easily found as the fully connected state $|2, 1\rangle$. In the following, we first give the exact result of a small system size $L = 3$, and then generalize this solution to arbitrary sizes.

For $L = 3$ there are five possible fully connected states, where we have excluded the trivial state $|1, 2, 3\rangle$ as it is decoupled from the right chiral Haldane phase. One can show this by looking at the resulting states starting from the right chiral Haldane phase, and these states should have at least one singlet bond connecting the nearby sites. The ground state can then be expanded using these five

states as

$$|\psi_3\rangle = A_1|3, 2, 1\rangle + A_2|1, 3, 2\rangle + A_3|2, 1, 3\rangle + A_4|2, 3, 1\rangle + A_5|3, 1, 2\rangle. \quad (3)$$

By solving the Schrödinger equation $H_c|\psi_3\rangle = E_3|\psi_3\rangle$ we find the coupled equations for these coefficients

$$\begin{cases} -A_5 - A_4 - 6A_1 = E_3A_1 \\ -A_4 - A_5 - 6A_2 = E_3A_2 \\ -A_4 - A_5 - 6A_3 = E_3A_3 \\ -2A_3 - 2A_2 - 2A_1 - 9A_4 = E_3A_4 \\ -2A_1 - 2A_3 - 2A_2 - 9A_5 = E_3A_5 \end{cases}. \quad (4)$$

Obviously, the above equations have symmetric solutions with $A_1 = A_2 = A_3$ and $A_4 = A_5$, and under this symmetry we find the energy obeys $\frac{2}{E_3+6} = \frac{(E_3+9)}{6}$, which gives us the exact ground state energy $E_3 = -(15 + \sqrt{57})/2$.

We now generalize to length L . Since we take into account the translational invariant of the system and consider the periodic boundary condition, it is more convenient to transform the Hamiltonian into momentum space as

$$H_C = -\frac{2}{L} \sum_{q,k,k',\sigma,\sigma'} \cos(k-k') \times a_{\frac{q}{2}+k,\sigma}^\dagger b_{\frac{q}{2}-k,-\sigma}^\dagger b_{\frac{q}{2}-k',-\sigma'} a_{\frac{q}{2}+k',\sigma'}. \quad (5)$$

Similar to the above $L = 3$ case, the ground state ansatz can be written as

$$\begin{aligned} |\psi\rangle &= \sum_{\{r_i\}} c_{\{r_i\}} |r_1 r_2 \dots\rangle \\ &= \sum_{\{r_i\}} c_{\{r_i\}} \cdot \sum_{k_1,\sigma_1,k'_1,\sigma'_1,\dots} a_{k_1,\sigma_1}^\dagger b_{k'_1,\sigma'_1}^\dagger a_{k_2,\sigma_2}^\dagger b_{k'_2,\sigma'_2}^\dagger \dots \\ &\quad \times e^{i(k_1+k'_1 r_1)} e^{i(2k_2+k'_2 r_2)} \dots |0\rangle, \end{aligned} \quad (6)$$

where the summation is over all possible configurations of the SU(3) singlet bonds labeled as $\{r_i\}$. The coefficients $c_{\{r_i\}}$ can be determined through

$$\begin{aligned} &H_C |r_1 r_2 \dots\rangle \\ &= -N \sum_i (\delta_{i-r_i-1,0/-L} + \delta_{i-r_i+1,0/L}) |\dots r_i \dots\rangle \\ &\quad - \sum_{i \neq j} (\delta_{i-r_j-1,0/-L} + \delta_{i-r_j+1,0/L}) |\dots r_j \dots r_i \dots\rangle \\ &= -N \sum_i (\delta_{i-r_i-1,0/-L} + \delta_{i-r_i+1,0/L}) |r_1 r_2 \dots\rangle \\ &\quad - \sum_{i \neq j} (\delta_{i-r_j-1,0/-L} + \delta_{i-r_j+1,0/L}) |\dots r_j \dots r_i \dots\rangle, \end{aligned}$$

where $N = 3$ for a SU(3) system. Thus we get the cou-

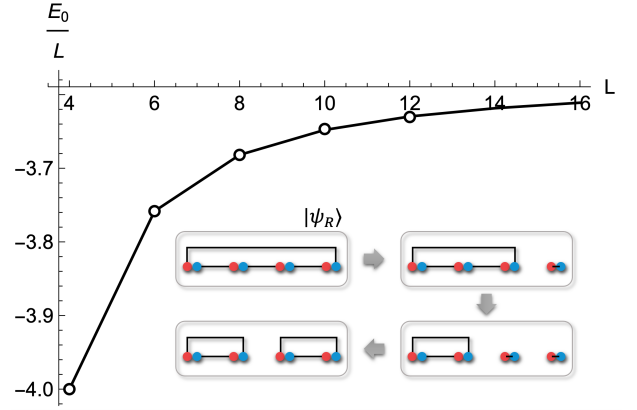


FIG. 5. Ground state energy density at the critical point for different system sizes L . The open points are results from the coupled Eqs. (7), and the solid line shows the DMRG results. The inset illustrates four substates in the ground state of the $L = 4$ system, with blue and red points labeling the quark and antiquark states and solid lines representing the SU(3) singlet bonds.

pled equations for the coefficients

$$\begin{aligned} &E c_{r_1 r_2 \dots} \\ &= -N \sum_i (\delta_{i-r_i-1,0/-L} + \delta_{i-r_i+1,0/L}) c_{r_1 r_2 \dots} \\ &\quad - \sum_{i \neq j} (\delta_{i-r_i-1,0/-L} + \delta_{i-r_i+1,0/L}) c_{\dots r_j \dots r_i \dots} \\ &= - \sum_{ij} [1 + (N-1) \delta_{ij}] \\ &\quad \times (\delta_{i-r_i-1,0/-L} + \delta_{i-r_i+1,0/L}) c_{\dots r_j \dots r_i \dots} \end{aligned} \quad (7)$$

The above coupled equations are huge and hard to solve. For system size L , there are at most $L! - 1$ coefficients to find. However, we can always simplify these equations by the symmetry of the subspaces. For example, similar to the $L = 3$ case, we always have the coefficient of right chiral Haldane phase $|2, 3, 4, \dots, L, 1\rangle$ equals the one of the left chiral Haldane phase $|L, 1, 2, \dots, L-1\rangle$. The coupled equations can then be solved as follows. We start from the left and right chiral Haldane phases with other fully connected states unoccupied. After finding the energy E , we take into account the equations with states coupled with the occupied ones and find the corresponding coefficients. The energy is then updated with new occupied states. This procedure is carried out iteratively until we get the convergent ground-state energy. In Fig. 5 we show the ground state energy densities with above ansatz as the open points, which coincide well with the DMRG results (solid line). This justifies our description of the critical point.

We can now understand the breakdown of the entanglement spectrum degeneracy at this point. As illustrated

in the inset of Fig. 5, the redistribution of these singlet bonds leads to subspaces which are product states of the left and right subsystems. Occupation of these states lifts the entanglement spectrum degeneracy, and leads this system to a critical point. This also explains why the positive t in Eq. (1) is crucial to realize the SU(3) Haldane phase, since this term suppresses the hopping of quark/antiquark states that leads to the product states as shown by the gray arrows in Fig. 5, and thus stabilizes the Haldane phase.

To conclude, I have proposed an experimentally feasible cold atomic system to realize the non-trivial Haldane phase with SU(3) symmetry. I show how to construct species-dependent zigzag optical lattices to reach the SU(3) adjoint representation with two spinor Bose gases. I find this SU(3) Haldane phase is connected to a critical one, and explains the break of entanglement spectrum degeneracy at this point. Finally, I mention the related experimental observations. The different edge states of the Haldane phase can be directly observed by quantum gas microscopes, as well as its string order parameters [41]. A Protocol for measuring the entanglement spectrum in cold atomic systems has been proposed [42], however the experimental realization might still be challenging.

This research is supported by FRFCU (No. FRF-TP-19-013A3).

* jxu@ustb.edu.cn

- [1] F. D. M. Haldane, Phys. Lett. A **93**, 464 (1983); Phys. Rev. Lett. **50**, 1153 (1983).
- [2] I. Affleck, T. Kennedy, E. H. Lieb, and H. Tasaki, Phys. Rev. Lett. **59**, 799 (1987).
- [3] I. Affleck, J. Phys.: Condens. Matter **1**, 3047 (1989).
- [4] Z. Gu and X. Wen, Phys. Rev. B **80**, 155131 (2009).
- [5] F. Pollmann, A. M. Turner, E. Berg, and M. Oshikawa, Phys. Rev. B **81**, 064439 (2010).
- [6] F. Pollmann, E. Berg, A. M. Turner, and M. Oshikawa, Phys. Rev. B **85**, 075125 (2012).
- [7] M. Lajkó, K. Wamer, F. Mila, and I. Affleck, Nucl. Phys. B **924**, 508 (2017).
- [8] K. Wamer, M. Lajkó, F. Mila, and I. Affleck, Nucl. Phys. B **952**, 114932 (2020).
- [9] M. Greiter, S. Rachel, and D. Schuricht, Phys. Rev. B **75**, 060401(R) (2007).
- [10] M. Greiter and S. Rachel, Phys. Rev. B **75**, 184441 (2007).
- [11] S. Rachel, R. Thomale, M. Führinger, P. Schmitteckert, and M. Greiter, Phys. Rev. B **80**, 180420(R) (2009).
- [12] K. Wamer and I. Affleck, Phys. Rev. B **101**, 245143 (2020).
- [13] T. Morimoto, H. Ueda, T. Momoi, and A. Furusaki, Phys. Rev. B **90**, 235111 (2014).
- [14] I. Affleck, D. Bykov, and K. Wamer, Phys. Rep. **953**, 1 (2022).
- [15] S. Gozel, P. Nataf, and F. Mila, Phys. Rev. Lett. **125**, 057202 (2020).
- [16] L. Devos, L. Vanderstraeten, and F. Verstraete, Phys. Rev. B **106**, 155103 (2022).
- [17] K. Wamer, F. H. Kim, M. Lajkó, F. Mila, and I. Affleck, Phys. Rev. B **100**, 115114 (2019).
- [18] S. Rachel, D. Schuricht, B. Scharfenberger, R. Thomale, and M. Greiter, J. Phys.: Conf. Ser. **200**, 022049 (2010).
- [19] S. Gozel, D. Poilblanc, I. Affleck, and F. Mila, Nucl. Phys. B **945**, 114663 (2019).
- [20] M. A. Cazalilla and A. M. Rey, Rep. Prog. Phys. **77**, 124401 (2014).
- [21] H. Nonne, M. Moliner, S. Capponi, P. Lecheminant, and K. Totsuka, Europhys. Lett. **102**, 37008 (2013).
- [22] V. Bois, S. Capponi, P. Lecheminant, M. Moliner, and K. Totsuka, Phys. Rev. B **91**, 075121 (2015).
- [23] H. Ueda, T. Morimoto, and T. Momoi, Phys. Rev. B **98**, 045128 (2018).
- [24] M. Mathur and D. Sen, J. Math. Phys. **42**, 4181 (2001).
- [25] S. Chaturvedi and N. Mukunda, J. Math. Phys. **43**, 5262 (2002).
- [26] R. Anishetty, M. Mathur, and I. Raychowdhury, J. Math. Phys. **50**, 053503 (2009).
- [27] Y. Kawaguchi and M. Ueda, Phys. Rep. **520**, 253 (2012).
- [28] H. Yang and H. Katsura, Phys. Rev. Lett. **122**, 053401 (2019).
- [29] M. Theis, G. Thalhammer, K. Winkler, M. Hellwig, G. Ruff, R. Grimm, and J. Hecker Denschlag, Phys. Rev. Lett. **93**, 123001 (2004).
- [30] C. D. Hamley, E. M. Bookjans, G. Behin-Aein, P. Ahmadi, and M. S. Chapman, Phys. Rev. A **79**, 023401 (2009).
- [31] D. J. Papoular, G. V. Shlyapnikov, and J. Dalibard, Phys. Rev. A **81**, 041603(R) (2010).
- [32] G. Grynberg and C. Robilliard, Phys. Rep. **355**, 335 (2001).
- [33] J. Ruostekoski, G. V. Dunne, and J. Javanainen, Phys. Rev. Lett. **88**, 180401 (2002).
- [34] D. McKay and B. DeMarco, New J. Phys. **12**, 055013 (2010).
- [35] D. Jaksch and P. Zoller, New J. Phys. **5**, 56 (2003).
- [36] M. Aidelsburger, M. Atala, S. Nascimbène, S. Trotzky, Y. A. Chen, and I. Bloch, Phys. Rev. Lett. **107**, 255301 (2011).
- [37] H. Miyake, G. A. Siviloglou, C. J. Kennedy, W. C. Burton, and W. Ketterle, Phys. Rev. Lett. **111**, 185302 (2013).
- [38] M. Cohen. and T. Feldmann, J. Phys. B: At. Mol. Phys. **15**, 2563 (1982).
- [39] W. Greiner and B. Müller, *Quantum Mechanics: Symmetries* (Springer, Berlin, 1994).
- [40] H. Georgi, *Lie Algebras in Particle Physics* (Westview, Boulder, 1999).
- [41] P. Sompet, S. Hirthe, D. Bourgund, T. Chalopin, J. Bibo, J. Koepsell, P. Bojović, R. Verresen, F. Pollmann, G. Salomon, C. Gross, T. A. Hilker, and I. Bloch, Nature **606**, 484 (2022).
- [42] H. Pichler, G. Zhu, A. Seif, P. Zoller, M. Hafezi, Phys. Rev. X **6**, 041033 (2016).